

Article

DOI: 10.18500/0869-6632-2022-30-3-299-310

Compartmental spiking neuron model CSNM

A. V. Bakhshiev✉, A. A. Demcheva

Peter the Great St. Petersburg Polytechnic University, Russia

E-mail: ✉palexab@gmail.com, ademtcheva@gmail.com

Received 7.11.2021, accepted 20.12.2021, published 31.05.2022

Abstract. The *purpose* of this work is to develop a compartment spiking neuron model as an element of growing neural networks. *Methods.* As part of the work, the CSNM is compared with the Leaky Integrate-and-Fire model by comparing the reactions of point models to a single spike. The influence of hyperparameters of the proposed model on neuron excitation is also investigated. All the described experiments were carried out in the Simulink environment using the tools of the proposed library. *Results.* It was concluded that the proposed model is able to qualitatively reproduce the reaction of the point classical model, and the tuning of hyperparameters allows reproducing the following patterns of signal propagation in a biological neuron: a decrease in the maximum potential and an increase in the delay between input and output spikes with an increase in the size of the neuron or the length of the dendrite, as well as an increase in the potential with an increase in the number of active synapses. *Conclusion.* The proposed compartment spiking neuron model allows to describe the behavior of biological neurons at the level of pulse signal conversion. The hyperparameters of the model allow tuning the neuron responses at fixed other neuron parameters. The model can be used as a part of spiking neural networks with details at the level of compartments of neurons dendritic trees.

Keywords: neuromorphic systems, spiking neural network, spiking neuron, compartment neuron model.

For citation: Bakhshiev AV, Demcheva AA. Compartmental spiking neuron model CSNM. Izvestiya VUZ. Applied Nonlinear Dynamics. 2022;30(3):299–310. DOI: 10.18500/0869-6632-2022-30-3-299-310

This is an open access article distributed under the terms of Creative Commons Attribution License (CC-BY 4.0).

Introduction

In the last decade, the theory and practice of artificial neural networks have achieved a number of significant results in solving machine learning problems [1]. However, the question of creating hardware energetically efficient neuromorphic calculators is still open [2]. The development of hardware implementations of spiking neural networks is one of the promising solutions to this problem [3].

Despite the successes achieved, deep neural networks are experiencing a number of problems associated with limited generalizing ability, especially in a changing environment [4]. Therefore, the study of the structure and principles of functioning of the nervous system in order to propose new architectures and methods of training artificial neural networks remains relevant. In this direction, the use of spiking models of neurons and neural networks is promising both for describing the behavior of natural neural structures and for modeling neuromorphic control and information processing systems.

Currently, spiking neural networks use fairly simple, point-based models of neurons. Such as the threshold integrator model (Integrate-and-Fire, Iaf) and its modifications, the Izhikevich model, SRM₀ (Simple Spike Response Model) [5], as well as relatively simple models of synaptic

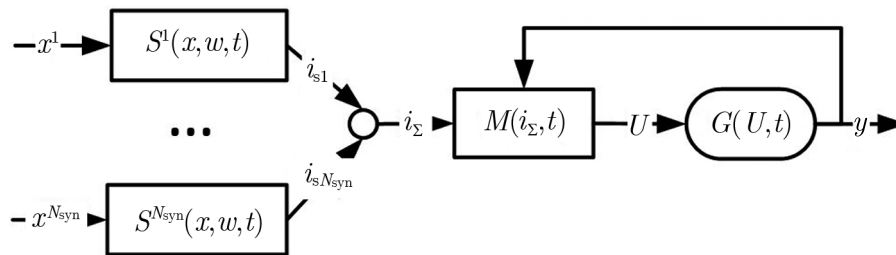


Fig. 1. Функциональная схема точечных моделей нейронов

Fig. 1. Functional diagram of point neuron models

transmission [6, 7]. A point spiking model of a neuron as an element of a neural network can be represented by the following functional scheme (Fig. 1)

In the diagram $S(x, w, t)$ – functional recording of the synaptic transmission model, which converts the input signal into synaptic current; $M(i_{\Sigma}, t)$ – functional recording of the membrane model, which performs spatial and temporal summation of input signals; $G(U, t)$ – an action potential generator that generates an output signal in response to the U potential of a neuron exceeding a certain threshold value.

More complex biophysical models of the neuron membrane (for example, the Hodgkin-Huxley model [8]) are not used due to the high computational complexity.

In nature, one of the main ways to achieve plasticity of the nervous system, which is not taken into account by point models, is the growth of the dendritic tree and the synaptic apparatus of the neuron involved in memorizing information and forming new patterns of activity. To describe the complex structure of the neuron membrane, there is a cable theory [9] and segment models of neurons [10]. However, they are also computationally complex and not quite convenient for modeling spike neural networks.

In the works [11, 12], a segmental spike model of a neuron was presented. Its feature is the ability to form the required neuron response, operating with such hyperparameters as the size of the neuron, the length of dendrites, the number of excitatory or inhibitory synapses, without switching to parametric tuning of each element. The model was used to study control and information processing systems based on models of neural networks close to biology [13]. The disadvantage of this model is the incompatibility of functional elements (synapse, membrane segment, low-threshold zone) in inputs and outputs with classical models. The implementation of a pulse generator to stabilize the duration of the output pulse contains an additional non-adaptive inertial link that negatively affects the overall inertial properties of the neuron.

In this paper, we present an updated segmental Spike Neuron Model (Compartment Spiking Neuron Model – CSNM), free from these shortcomings.

1. Neuron model

1.1. Model Architecture. The model is based on the equivalent electrical circuit of the membrane according to Eccles (Fig. 2) [14]. Here R_m – membrane resistance, C_m – membrane capacity, R_s – synapse resistance, E_m and E_s – Membrane EDS and synaptic transmission.

In the CSNM model, we abstract from the quantitative description of chemical processes in a neuron and from the concept of ion channels. In order to preserve the ability to describe the complex dynamics of the integration of input signals on the membrane, we introduce the concept of ionic mechanisms, which can be, in general, an arbitrary number, and processes in which generally correspond to the dynamics of the circuit in Fig. 2.

On fig. 3 a structural description of the neuron membrane segment of the proposed model is

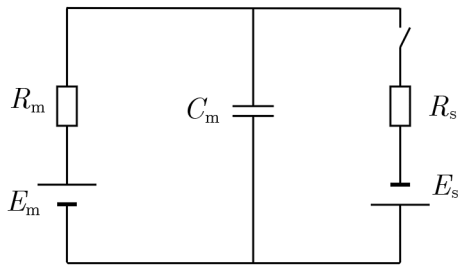


Fig. 2. Эквивалентная электрическая схема мембраны по Экклсу

Fig. 2. Eccles membrane equivalent electric diagram

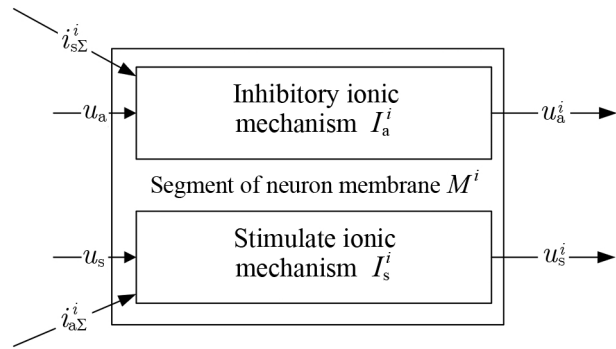


Fig. 3. Структура ионного механизма сегмента мембраны нейрона

Fig. 3. Structure of neuron membrane segment ion mechanism

presented. Here $i_{a\Sigma}^i$ – total effect of inhibitory synapses, $i_{s\Sigma}^i$ – total effect of excitatory synapses, u_a^i – inhibitory (negative) contribution to the potential of the neuron, u_s^i – excitatory (positive) contribution to the potential of the neuron. Excitatory synapses $i_{s\Sigma}^i$ have an effect on the inhibitory ion mechanism i_a , and inhibitory $i_{a\Sigma}^i$ – on the excitatory i_s . Thus, the synapse weakens the normal function of the ion mechanism.

In Fig. 4 the structural and functional diagram of the model is presented [12].

The following designations are accepted in the diagram: $B^1 \dots B^{N_s}$ – segments of the neuron body membrane; N_s – the size of the neuron body; $D^{1,1} \dots D^{L, N_d(L)}$ – dendritic tree membrane segments; N_d – dendrite length; L – number of dendrites; $S^1 \dots S^{N_{syn}}$ – synapses (the subscript defines the excitatory synapse (s), or inhibitory (a)); N_{syn} – the number of synapses formed on the segment of the dendrite; $x_s^1 \dots x_s^{N_{syn}}$ – input signal (pulse sequence) arriving at synapses; $i_{a\Sigma}^n$, $i_{s\Sigma}^n$ – total effect of inhibitory and excitatory synapses; E_m – initial state of ion mechanisms at rest; $U^1 \dots U^{N_s}$ – contributions of body membrane segments to the total potential of the neuron; U_Σ – total potential of the neuron; Y – output signal (pulse sequence) generated by the neuron.

Neurons exchange information through events-impulses (spikes), which can be represented as:

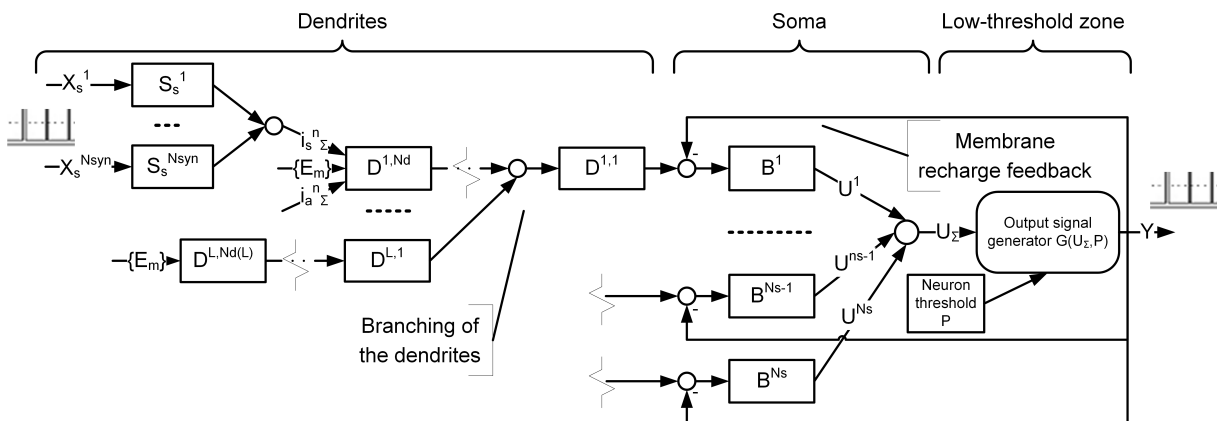


Fig. 4. Структурно-функциональная схема модели нейрона

Fig. 4. Structural and functional diagram of the neuron model

$$x = \begin{cases} E_y, & t_i \leq t \leq t_i + \Delta t, \\ 0, & t < t_i, t > t_i + \Delta t, \end{cases} \quad (1)$$

where E_y is the amplitude of the input pulse, t_i is the start time of the formation of the input pulse, Δt is the duration of the input pulse.

The x pulses arriving at the input of synapses are converted into an output value that simulates the effect of synaptic current on a segment of the neuron membrane. The segments of the membrane of the neuron body and dendrites are pairs of ionic mechanisms describing the mechanisms of depolarization and hyperpolarization. The output of the membrane segment is a pair of hyperpolarization and depolarization values, which determines their contribution to the total potential.

The action potential generator generates an output pulse that can be transmitted to other neurons in the network. It also generates a feedback signal to the segments of the cell body membrane, which makes it possible to describe transients that occur during pulse generation.

Such a structural organization of the neuron model makes it possible to calculate systems of differential equations for each neuron independently, since neurons exchange exclusively information about the moment of pulse occurrence, and the input vector of the system of equations of the neuron model is formed inside the model as a function of the moments of pulse arrival.

The system as a whole is characterized by a set of the following hyperparameters: the size of the neuron N_s (the number of blocks-models of the membrane segment), the length of the dendrites N_d and the number of excitatory or inhibitory synapses (the number of corresponding blocks in the model) N_{syn} . Their values set the overall appearance of the system and allow you to form the required neuron response.

Next, the mathematical description of models of functional elements of a neuron is considered.

1.2. Synaptic transmission model. The input of the synapse model (2) receives a signal from the output of a presynaptic neuron of the form (1). A synaptic current is formed at the output of the synapse model. The synapse model implements the main features of the functioning of synaptic transmission — the exponential nature of the release and decay of the mediator, the difference in the rates of these processes and the effect of presynaptic inhibition. The models of excitatory and inhibitory synapses are identical to each other. The difference in their effect on the membrane segment is determined by which of the ion mechanisms each specific synapse is connected to.

Equations of the synapse model:

$$\left. \begin{aligned} T_s(t) \frac{d\rho}{dt} &= x - \rho(t) \\ g &= F_{PreI}(\rho) \\ i_s &= g \frac{\varepsilon_s}{R_s} w \end{aligned} \right\}, \quad (2)$$

where $R_s > 0$ — synapse resistance, ε_s — electromotive force (EMF) of synaptic transmission, g — time variable describing synapse activity taking into account the effect of presynaptic inhibition, w — the weight of the connection, i_s — the output synaptic current, ρ — characterizes the conditional concentration of the mediator released in response to the pulse. Initial conditions: $\rho(0) = 0$.

In the equation above, $T_s(t)$ is a time constant defined by the formula

$$T_s(t) = \begin{cases} \tau_s, & x(t) > 0, \\ \tau_d, & x(t) \leq 0, \end{cases} \quad (3)$$

where τ_s is the mediator release time constant, τ_d is the mediator decay time constant. $F_{\text{PreI}}(\rho)$ — a function simulating the effect of presynaptic inhibition, described as:

$$F_{\text{PreI}}(\rho) = \max \left(0, \begin{cases} 4\zeta(\rho - \zeta\rho^2), & \zeta \geq 0.5 \\ \rho, & \zeta = 0 \end{cases} \right), \quad (4)$$

where $\zeta \in 0, [0.5, \infty)$ — the critical value of the mediator concentration at which the effect of presynaptic inhibition begins to affect (zero value means refusal to use the effect of presynaptic inhibition).

Note that in this model, both its physical parameters R_s and ε_s and the weight of w contribute to the measure of the effectiveness of the impact of the synapse on the membrane segment. This is due to the unification of the use of the synapse model — in the neural network parameter optimization mode (for example, according to the STDP rule — Spike-timing dependent plasticity), the weight w is modified. In the mode of structural adaptation, the weight of the synapse is assumed to be equal to one. In any case, the physical parameters of the model are selected based on the specifics of the simulated structure of connections.

The ionic mechanism of the neuron membrane is directly affected by the synaptic current i_s , proportional to the effective conductivity of the synapse.

1.3. Model of the ion mechanism of the membrane segment. In the works [11, 12], a model of the ion mechanism is proposed, which has three main characteristics: resistance R_m , capacity C_m and ion concentration E_m , supported by the pumping function of the channel inside the cell. The product $T_m = R_m C_m$ characterizes the inertia of the channel at rest, that is, the rate of restoration of the normal concentration of ions in the cell.

The model of the ion mechanism reflects the change in the membrane potential depending on the influence of the synapse, which consists in the loss of the efficiency of the pumping function of the channel and in a decrease in the concentration of ions in the cell with a time constant of this process $T(t) = R^I(t)C_m$.

The resistance of $R^I(t)$ is determined from the relation

$$\frac{1}{R^I(t)} = \frac{i_{s1}(t)}{\varepsilon_{s1}} + \frac{i_{s2}(t)}{\varepsilon_{s2}} + \dots + \frac{i_{sn}(t)}{\varepsilon_{sn}} + \frac{1}{R_m} = g_{\Sigma}(t) + \frac{1}{R_m}, \quad (5)$$

where $i_{s1}(t), i_{s2}(t), \dots, i_{sn}(t)$ — synaptic currents of active synapses acting on this ionic mechanism; $\varepsilon_{s1}, \varepsilon_{s2}, \dots, \varepsilon_{sn}$ — Synapse EMF; $g_{\Sigma}(t) = i_{s\Sigma}(t)/\varepsilon_s$ — total conductivity of active synapse models, $i_{s\Sigma}(t)$ — total synaptic current, $R_m > 0$ — membrane resistance. Next, we assume that the EMF of all synapses are equal.

The corresponding system of equations is given below.

$$\left. \begin{aligned} T_I \frac{du}{dt} &= u_{\Sigma} - (1 + g_{\Sigma}R_m)u \\ T_I &= \frac{C_m}{g_{\Sigma} + R_m^{-1}} \end{aligned} \right\}, \quad (6)$$

where $u_{\Sigma}(t)$ — the expected contribution of the segment to the value of the intracellular potential in the absence of external excitation, which is determined by the activity of the previous segments of the membrane, $u(t)$ — the real contribution of the segment to the value of the intracellular potential. Initial conditions: $u(0) = 0$.

The membrane segment model structurally consists of one or more ionic mechanisms and synapses. Each segment has two input vectors — synaptic inputs X and expected contributions to the membrane potential U_{Σ} , and one output vector U .

1.4. Model of the output signal generator. Another important link of the model under consideration is an output signal generator that generates events about the generation of a neuron pulse. The value of the neuron output signal is determined by the following expression:

$$y = F_G(\bar{U}, P_{act}, P_{rest}), \quad (7)$$

where \bar{U} — the average value of the potential from the sections of the membrane of the neuron body, y — a signal (pulse) informing about the firing of the neuron, $F_G(\bar{U})$ — a hysteresis function that returns 1 when exceeding \bar{U} of the threshold P_{act} , and 0 if the value of \bar{U} becomes below the threshold P_{rest} . The generated output signal y enters the feedback of the recharge of the neuron body, which makes it possible to describe the effects of absolute and relative refractoriness, as well as residual depolarization of the neuron after pulse generation.

1.5. The system of equations of the neuron model. The system of equations describing the neuron model contains N first-order differential equations, where N is calculated by the formula

$$N = \sum_{i=1}^L \left(1 + L_D^i + N_B^i + \sum_{l=1}^{L_D^i} N_l^i \right), \quad (8)$$

where L — the number of segments of the neuron body, L_D^i — the number of segments of the dendrite corresponding to the i th segment of the body, N_B^i — the total number of excitatory and inhibitory synapses per i -th segment of the neuron body, N_l^i — the total number of excitatory and inhibitory synapses on the l -th segment of the dendrite of the i -th segment of the neuron body.

Thanks to the accepted model of input and output signals, with a numerical solution, such a system of equations can be divided into N independent first-order differential equations at each step of the calculation, stitched together according to boundary conditions at the start or end of the input and output pulses. In addition, the equations of the synapse models become linear. Thus, the numerical calculation of the entire neural network can be implemented as a calculation of a system of independent differential equations of the first order.

1.6. Model Parameters. The table shows the values of the model parameters of all functional elements of the neuron. The values of the parameters were chosen in such a way as to demonstrate most clearly the possibilities of a qualitative description of the reactions of natural neurons with different structural organization of the membrane.

2. Experiments

The section describes the results of mathematical and numerical modeling based on model CSNM. The experiments were carried out in the Matlab Simulink environment using the tools of the block library proposed by the authors. The parameters of the blocks are set by default in accordance with the Table, unless otherwise specified in the description of the experiment. The numerical solution is obtained using the explicit Runge–Kutta method with variable pitch. The library itself, as well as the blocks and diagrams used in the experiments, are available at the link [15].

2.1. Analysis of the reactions of the point model to a single pulse. To compare the proposed model with the classical model of the threshold integrator, a simulation of the reaction to the pulse action was performed.

A single input effect was set for both models. At the output, dependences on the time of the membrane potential as a reaction to the received pulse were obtained. In Fig. 5 the simulation

Таблица. Значения параметров модели нейрона
Table. Values of neuron model parameters

Synapse
Mediator allocation time constant $\tau_s = 0.001c$
Mediator decay time constant $\tau_d = 0.005c$
The amplitude of the input signal $E_y = 1$
The coefficient of influence of the presynaptic inhibition effect $\zeta = 1$
Equivalent synapse resistance («weight» synapse) $R_s = 2 \cdot 10^7 \text{ Ом}$
The EMF of synaptic transmission $\varepsilon_s = -0.07 \text{ In}$
Ionic membrane mechanism
Equivalent resistance of the membrane at rest $R_0 = 1 \cdot 10^7 \text{ Ом}$
Equivalent resistance in the recharge state $R_F = 1 \cdot 10^7 \text{ Ом}$
Equivalent membrane capacity $C_m = 1 \cdot 10^{-9} \text{ Ф}$
Initial contributions $\{E\} = \{E^+, E^-\}$ to the membrane potential of ion mechanisms at rest: $E_m^+ = 0.93, E_m^- = -1$
Action Potential Generator
Neuron activation threshold $P_{\text{on}} = -0.055 \text{ In}$
Neuron deactivation threshold $P_{\text{off}} = -0.1 \text{ In}$
The time constant that determines the inertia of the generator mechanism $T_G = 0.005s$
The amplitude of the output signal $E_y = 1$
Feedback coefficient $F = 2$

results are shown. The membrane potential graphs for the two models under consideration are similar in terms of limiting amplitudes and time delays. Qualitative differences in the shape of the pulse are determined by the difference in the mathematical description of the models (a different model of the membrane and the generator of the action potential in the model CSNM).

Experiments were conducted to study the behavior of the model depending on the structural parameters. For the experiments, the threshold of the neuron was artificially inflated to exclude the generation of output pulses. Thus, the dependences of the peak value of the potential amplitude on the body size N_s and the length of the dendrite were obtained (Fig. 6), on the number of active synapses N_{syn} (рис. 7).

According to the experimental results, it can be seen that with the same input effect, the peak amplitude of the potential of a larger neuron ($N_s > 1$) decreases nonlinearly. A similar pattern is observed when the length of the dendrite changes — the longer the dendrite through which the exciting signal was transmitted, the smaller the peak potential with the same input effect. An increase in the number of active synapses N_{syn} contributes to an increase in the peak amplitude of the neuron potential.

In Fig. 8 shows the dependence of the delay in the formation of the output pulse on the

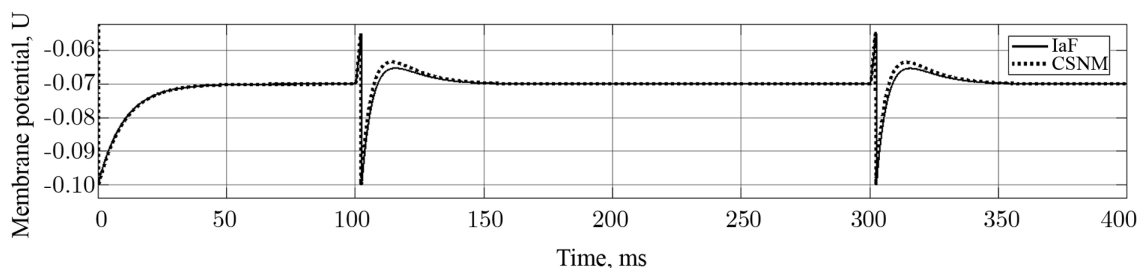


Fig. 5. Сравнение реакций моделей CSNM и IaF на одиночный импульс

Fig. 5. Comparison of reactions of CSNM and IaF models to a single spike

location of the synapse (or otherwise — the length of the dendrite N_d) and the size of the neuron N_s . Thus, we can conclude that it is possible to optimize the structure of the neuron for the input patterns of impulses. In this case, the parameter N_s will determine the overall inertia of the neuron, N_d — the amount of delay in triggering upon the arrival of a signal on this dendrite, N_{syn} — the amplitude of the potential (and as a consequence — the frequency of the output pulses).

The ability of the proposed model to structural adaptation, together with the patterns observed in experiments, make it possible to use CSNM to solve image recognition problems. So,

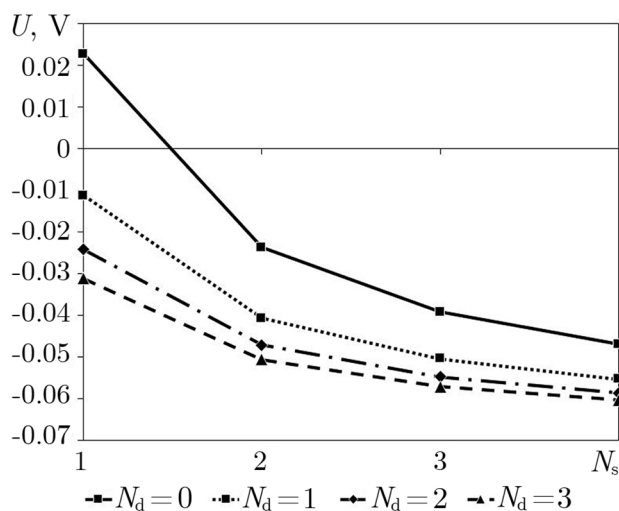


Fig. 6. Зависимость пикового значения амплитуды потенциала от размера тела нейрона при различных длинах дендрита

Fig. 6. Dependence of the peak potential amplitude on the neuron body size at different dendrite lengths

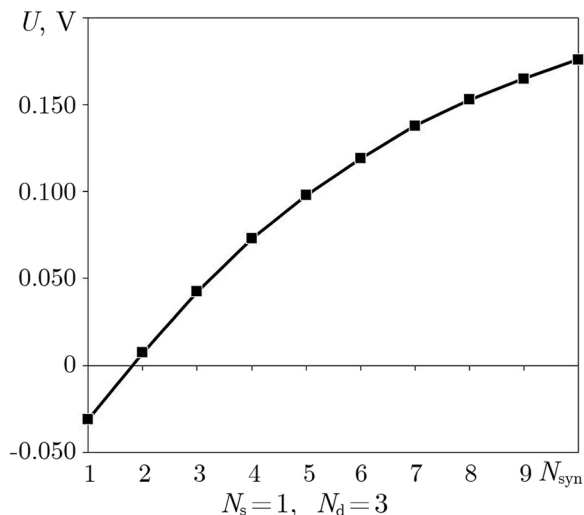


Fig. 7. Зависимость пикового потенциала нейрона от числа активных синапсов

Fig. 7. Dependence of the peak potential on the number of active synapses

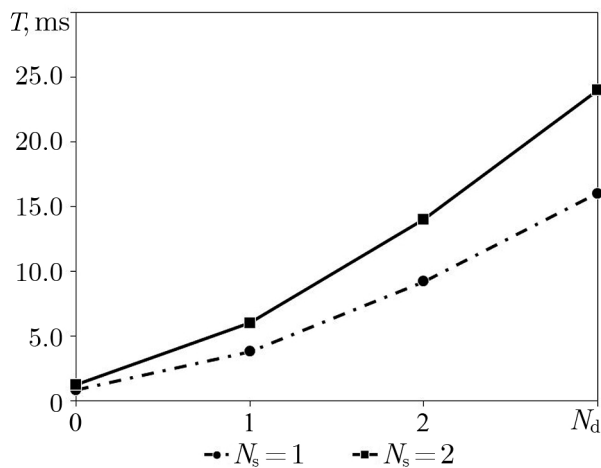


Fig. 8. Зависимость времени задержки между входным и выходным импульсами от длины дендрита и размера нейрона

Fig. 8. Dependence of the delay time between the input and output spikes on the length of the dendrite and the size of the neuron

in the work [16], an algorithm for structural training of a neuron model to recognize a pattern of impulses was implemented.

Conclusion

The proposed segmental spike model of a neuron allows us to qualitatively describe the behavior of biological neurons at the level of the dynamics of the transformation of pulse flows. However, the question of model verification on real biological objects remains open. The hyperparameters of the model (the number of body segments, the length of dendrites, the number of synapses) allow you to adjust the reactions of the neuron with fixed other parameters. Such a model can be used as an element of spike neural networks with detailing up to the level of segments of dendritic trees of neurons. As part of further research, work is underway to create an architecture and algorithms for structural learning of segmented spike neural networks for solving machine learning problems. In the future, it is planned to create hardware implementations of segment spike neural networks.

References

1. Shrestha A, Mahmood A. Review of deep learning algorithms and architectures. *IEEE Access*. 2019;7:53040–53065. DOI: 10.1109/ACCESS.2019.2912200.
2. James CD, Aimone JB, Miner NE, Vineyard CM, Rothganger FH, Carlson KD, Mulder SA, Draelos TJ, Faust A, Marinella MJ, Naegle JH, Plimpton SJ. A historical survey of algorithms and hardware architectures for neural-inspired and neuromorphic computing applications. *Biologically Inspired Cognitive Architectures*. 2017;19:49–64. DOI: 10.1016/j.bica.2016.11.002.
3. Tavanaei A, Ghodrati M, Kheradpisheh SR, Masquelier T, Maida A. Deep learning in spiking neural networks. *Neural Networks*. 2019;111:47–63. DOI: 10.1016/j.neunet.2018.12.002.
4. Marcus G. Deep Learning: A Critical Appraisal [Electronic resource]. arXiv:1801.00631. arXiv Preprint; 2018. 27 p. Available from: <https://arxiv.org/abs/1801.00631>.
5. Gerstner W. Population dynamics of spiking neurons: Fast transients, asynchronous states, and locking. *Neural Computation*. 2000;12(1):43–89. DOI: 10.1162/089976600300015899.
6. Gerstner W, Kistler WM. *Spiking Neuron Models: Single Neurons, Populations, Plasticity*. Cambridge: Cambridge University Press; 2002. 480 p. DOI: 10.1017/CBO9780511815706.
7. Izhikevich EM. Simple model of spiking neurons. *IEEE Transactions on Neural Networks*. 2003;14(6):1569–1572. DOI: 10.1109/TNN.2003.820440.
8. Hodgkin AL, Huxley AF. A quantitative description of membrane current and its application to conduction and excitation in nerve. *Bulletin of Mathematical Biology*. 1990;52(1–2):25–71. DOI: 10.1007/BF02459568.
9. Bell J. Cable theory. In: Binder MD, Hirokawa N, Windhorst U, editors. *Encyclopedia of Neuroscience*. Berlin, Heidelberg: Springer; 2009. DOI: 10.1007/978-3-540-29678-2_775.
10. Lindsay AE, Lindsay KA, Rosenberg JR. Increased computational accuracy in multi-compartmental cable models by a novel approach for precise point process localization. *Journal of Computational Neuroscience*. 2005;19(1):21–38. DOI: 10.1007/s10827-005-0192-7.
11. Bakhshiev AV, Romanov SP. Reproduction of the reactions of biological neurons as a result of modeling structural and functional properties membrane and synaptic structural organization. *Neurocomputers*. 2021;(7):25–35 (in Russian).
12. Bakhshiev A, Gundelakh F. Mathematical model of the impulses transformation processes in natural neurons for biologically inspired control systems development. In: Supplementary

Proceedings of the 4th International Conference on Analysis of Images, Social Networks and Texts (AIST-SUP 2015). Vol. 1452. Yekaterinburg, Russia, April 9–11, 2015. Aachen, Germany: CEUR-WS; 2015. P. 1–12.

13. Bakhshiev AV. Prospects for application of models of biological neural structures in the motion control system. *Information-measuring and Control Systems*. 2011;(9):85–90 (in Russian).
14. Eccles JC. *The Physiology of Synapses*. Berlin, Heidelberg: Springer; 1964. 316 p. DOI: 10.1007/978-3-642-64950-9.
15. Neuro Matlab: the spiking neuron models in Matlab Simulink [Electronic resource]. Available from: <https://github.com/aicomunity/NeuroMatlab>.
16. Bakhshiev AV, Korsakov AM, Astapova LA, Stankevich LA. The structural adaptation of the compartment spiking neuron model. In: *Proceedings of the VII All-Russian Conference «Nonlinear Dynamics in Cognitive Research — 2021»*. Nizhny Novgorod, 20–24 September 2021. Nizhny Novgorod: Institute of Applied Physics RAS; 2021. P. 30–33 (in Russian).